# Dramatic Substituent Effects on the Photoluminescence of Boron Complexes of 2-(Benzothiazol-2-yl)phenols

## Mithun Santra,[a] Hyunsoo Moon,[a] Min-Ho Park,[b] Tae-Woo Lee,*[b] Young Kook Kim,[c] and Kyo Han Ahn*[a]

**Abstract:** Substituents can induce dramatic changes in the photoluminescence properties of N,O-chelated boron complexes. Specifically, the boron complexes of 2-(benzothiazol-2-yl)phenols become bright deep blue- and orange-red-emitting materials depending on amino substituents at the 5- and 4-positions of 2-(benzothiazol-2-yl)phenol, respectively. Absorption and emission data show that the resulting boron complexes have little or small overlap between the absorption and emission spectra and, furthermore, X-ray crystal structures for both the blue and orange-red complexes indicate the absence of π–π stacking interaction in the crystal-packing structures. These features endow the boron complexes with bright and strong photoluminescence in the solid state, which distin-

guishes itself from the typical boron complexes of dipyrromethenes (BODI-PYs). A preliminary study indicates that the blue complexes have promising electro-optical characteristics as dopant in an organic light-emitting diode (OLED) device and show chromaticity close to an ideal deep blue. The substituent effects on the photoluminescent properties may be used to tune the desired emission wavelength of related boron or other metal complexes.

**Keywords:** absorption · boron · dyes/pigments · luminescence · substituent effects

## Introduction

Luminescent organic and organometallic compounds have attracted intense research interest on account of their potential applications in organic light-emitting diodes (OLEDs), solar cells, laser dyes, photosensitizers, biomolecular labels, and molecular probes. Among various types of luminescent compounds, boron complexes based on N- and O-donor ligands have received particular interest because they show excellent photophysical properties such as thermal and photochemical stability, high fluorescence quantum yield, and negligible triplet-state formation.[1] In particular, boron com-

plexes of dipyrromethenes, so-called BODIPYs, have been extensively explored for various applications.[2] BODIPY dyes can be considered N,N-chelated boron complexes of cyanine dyes in which electron delocalization between α- and ω-nitrogen donor/acceptor occurs through an oligomethine chain. The boron complexation results in the distinctive photochemical properties of BODIPY dyes relative to those of the cyanine dyes, which are also widely used for biological imaging. Accordingly, other conjugated dye molecules with donor and acceptor ligands that can form boron complexes would be of interest in the development of novel photoluminescent compounds. Indeed, N,N- and N,O-chelated boron complexes based on other types of organic dyes, which are also simply called BODIPY analogues,[3] have been explored in search of efficient photoluminescent and electroluminescent compounds.[4] Most of these boron complexes, however, show inferior photophysical properties to the conventional BODIPY dyes. Given that photoluminescent materials are useful for various applications, it would be of great value to develop new types of organoboron complexes with promising photophysical properties. Herein, we wish to disclose the dramatic substituent effects on the photoluminescent properties of N,O-chelated boron complexes, which resulted in bright blue- and orange-emitting complexes in solution and, furthermore, in the solid state. The substituent effects observed would also offer us an important guideline for the development of related photoluminescent and electroluminescent materials.

[a] M. Santra,[+] H. Moon,[+] Prof. K. H. Ahn
Department of Chemistry
Pohang University of Science and Technology (POSTECH)
San 31, Hyoja-dong, Pohang, 790-784 (Republic of Korea)
Fax: (+82) 54-279-5877
E-mail: ahn@postech.ac.kr

[b] M.-H. Park, Prof. T.-W. Lee
Department of Material Science and Engineering
Pohang University of Science and Technology (POSTECH)
San 31, Hyoja-dong, Pohang, 790-784 (Republic of Korea)
Fax: (+82) 54-279-2399
E-mail: twlee@postech.ac.kr

[c] Dr. Y. K. Kim
Next G. EVEN Development Team
Samsung Mobile Display
San 24, Nongseo-dong, Yongin, 446-811 (Republic of Korea)

[+] These authors contributed equally to this work.

Supporting information for this article is available on the WWW under http://dx.doi.org/10.1002/chem.201200726.

**WILEY** ONLINE LIBRARY

These are not the final page numbers! ↗↗

## Results and Discussion

In the course of our study on ratiometric fluorescent probes based on 2-(benzothiazol-2-yl)phenol (BTP) and its derivatives (Figure 1), we noticed that there are dramatic substituent effects on their emission properties.[5]
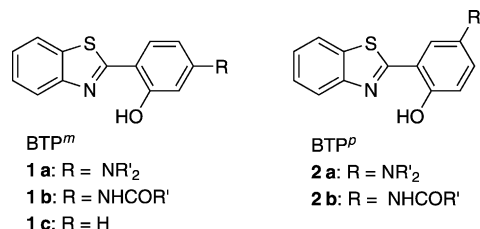


Figure 1. 2-(Benzothiazol-2-yl)phenol (BTP, **1c**) and its *meta*- and *para*-substituted derivatives.

Specifically, there were significant differences in the emission wavelengths between the *meta*- and *para*-substituted phenol derivatives **1b** and **2b** (R=NHCOCH₃; NHCOPh). Also, the *meta* derivatives **1b** showed hypsochromic shifts relative to the parent BTP **1c** (55 nm), whereas *para* analogues **2b** showed bathochromic shifts relative to **1c** (30 nm). These substituent effects prompted us to explore related BTP derivatives, in particular, amino derivatives **1a** and **2a**,[6] and the corresponding N,O-chelated boron complexes as novel photoluminescent materials.

**Synthesis**: The BTP derivatives with amine substituents at the *meta* and *para* positions can be synthesized in four and three steps starting from commercially available 2-amino-benzenethiol and 5-amino-2-hydroxybenzoic acid (for the *meta*-substituted derivatives) or 4-amino-2-hydroxybenzoic acid (for the *para*-substituted derivatives), respectively. A synthetic route for the *meta* derivatives is shown in Scheme 1. The *para* derivative **2a** (R′=Me) was synthesized according to the literature procedure.[6,7]

Then, we prepared the difluoroboron complexes **3** and **4** from the BTP^*m* and BTP^*p*, respectively (Figure 2), by treatment with boron trifluoride etherate in the presence of triethylamine. We also prepared diphenylboron analogues such
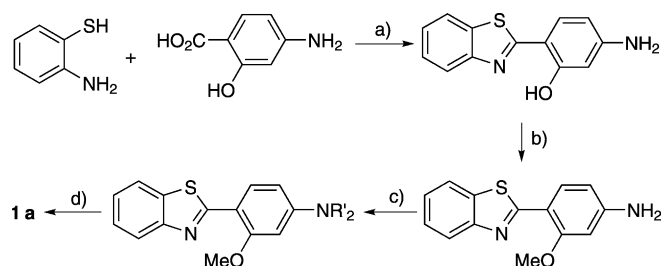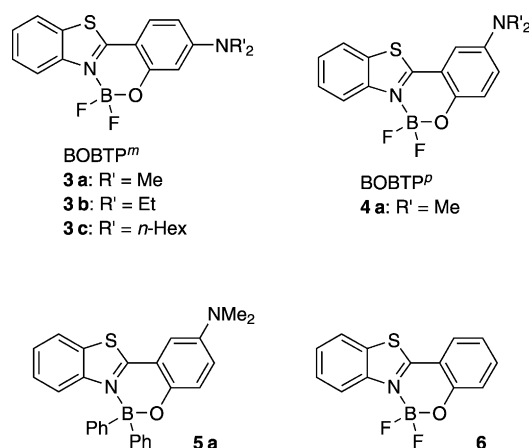


Figure 2. Boron complexes of 2-(benzothiazol-2-yl)phenol derivatives studied.

as **5a**,[8] but it was rather unstable in acetonitrile. Therefore, we focused on the difluoroboron complexes in the following studies. Details of the synthesis are described in the Supporting Information.

**Substituent effects**: The boron complexes of the BTP analogues, BOBTPs,[9] showed striking emission properties: for example, BOBTP^*m* **3a** (R′=Me) emitted strong blue luminescence ($\lambda_{em}$=430 nm) when excited at 395 nm in dichloromethane, whereas BOBTP^*p* **4a** (R′=Me) emitted orange luminescence ($\lambda_{em}$=597 nm) when excited at 450 nm in dichloromethane (Figure 2). The boron complexation thus leads to a larger shift in the emission wavelength (167 nm) depending on the substituent position relative to the case of the noncomplexed BTPs (55–85 nm). Thus, simply by changing the position of amino substituents, we were able to realize deep blue- and orange-emitting compounds in solution.

Both absorption and emission spectra of BOBTP^*m* **3a** and its *para* analogue **4a** are given in Figure 3. Both of the complexes emitted strongly when excited at the longest wavelength of the absorption maxima, 395 and 450 nm, respectively. BOBTP^*m* **3a** showed narrow absorption and emission bands similar to most of the BODIPY dyes, with the full widths at half-maximum (FWHM) of 40 and 39 nm, respectively, and with a small Stokes shift (17 nm). The *para* analogue **4a** showed an emission band with a larger value of FWHM (91 nm).

Interestingly, BOBTP^*m* dyes show small or little spectral overlap. For example, **3c** shows a relatively small absorption–emission spectral overlap despite a small Stokes shift (28 nm), as seen from the normalized spectra (Figure 4a). In the case of the *para* derivatives, BOBTP^*p* **4a**, there is a large Stokes shift (141 nm) with little spectral overlap (Figure 4b). Such low or small spectral overlap observed for the BOBTP dyes distinguishes them from the typical BODIPY dyes that show significant spectral overlap.[10]

BOBTP^*p* **4a** dissolves well in various organic solvents, whereas BOBTP^*m* **3a** has limited solubility in nonpolar solvents. Therefore, we varied the amino substituent (R′) of
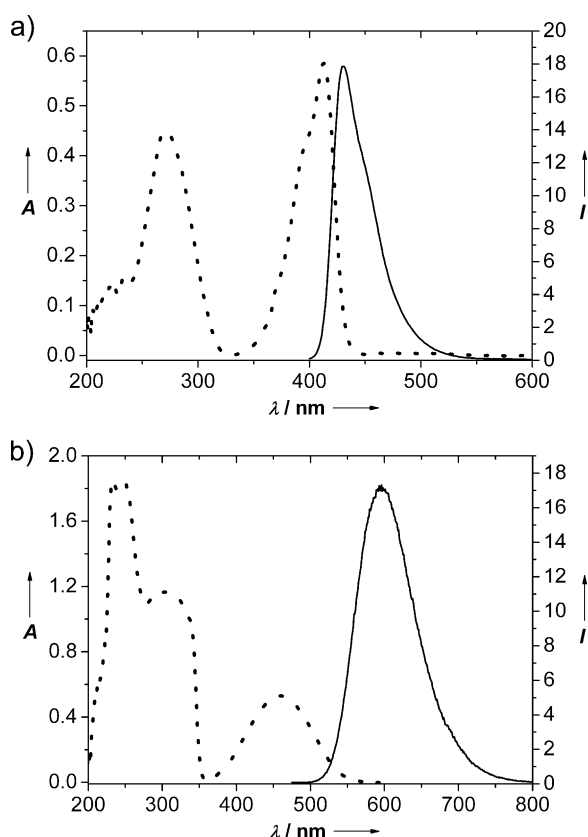


Scheme 1. Synthesis of BTPs **1a**. Reagents and conditions: a) polyphosphoric acid, 180°C; b) CH₃I, NaH, DMF, RT; c) CH₃CH₂Br or nC₆H₁₃Br, (nBu)₄N⁺I⁻, NaH, THF, reflux; d) nC₁₂H₂₅SH, NaOH, N-methyl-2-pyrrolidone (NMP), 130°C.

Figure 3. Electronic absorption (dotted line) and emission (solid line) spectra of a) BOBTP$^m$ **3a** (10 μM) and b) BOBTP$^p$ **4a** (100 μM) in dichloromethane.
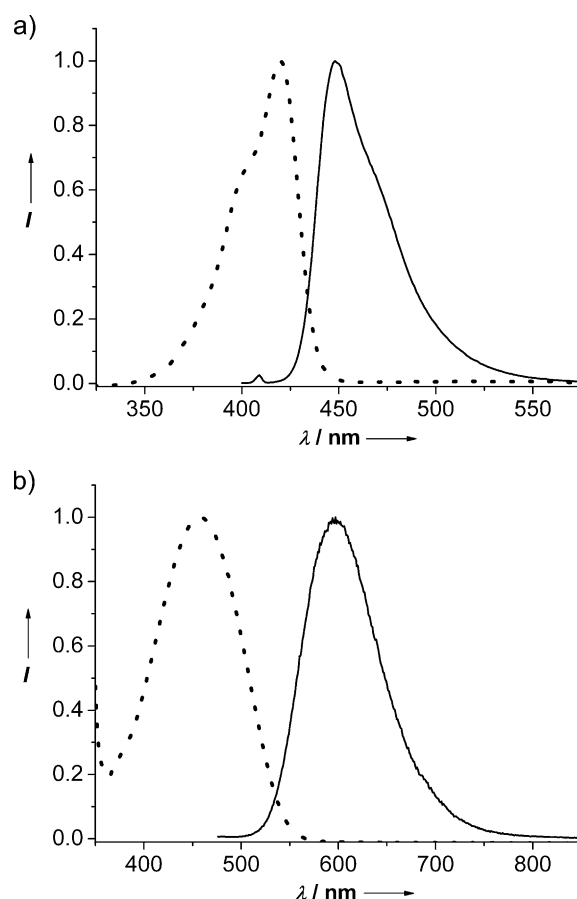


Figure 4. Normalized absorption (dotted line) and emission (solid line) spectra of a) BOBTP$^m$ **3c** and b) BOBTP$^p$ **4a** in dichloromethane.

BOBTP$^m$ to longer ones to enhance the solubility in various organic solvents. When the amino substituent in BOBTP$^m$ dyes was changed to longer alkyl groups, a slight bathochromic shift in the maximum emission wavelength resulted: (R′ = Me→Et→$n$-Hex: $\lambda_{em}$ = 430→434→448 nm; Figure 5). For a given BOBTP dye, the maximum emission wavelength showed small bathochromic shifts as the solvent polarity increased ($\lambda_{em}$ = 430–454 nm in the case of BOBTP$^m$ **3c**), along with substantial decrease in the emission intensity (Figure 6a). Such solvent-dependent behavior was also observed in the case of BOBTP$^p$ **4a** (Figure 6b).

Of particular note, BOBTP$^m$ dyes exhibit very bright and strong luminescence, which suggests that they might find potential applications in OLED materials. The photophysical properties of BOBTPs in solution are listed in Table 1.

A very high fluorescence quantum yield ($\Phi_F$ = 0.98 in cyclohexane) was obtained for BOBTP$^m$ **3c**, as determined with 9,10-diphenylanthracene as a reference dye ($\Phi_F$ = 0.90 in cyclohexane).[11] With a large molar extinction coefficient ($\varepsilon$ = 73000 M$^{-1}$cm$^{-1}$), BOBTP$^m$ **3** dyes thus constitute a promising class of blue-emitting boron complexes. The corresponding boron complex of the parent BTP ligand **1c** that lacks the 4-amino substituent, BOBTP **6** (Figure 2), is known to have a lower fluorescence quantum yield ($\Phi_F$ = 0.23 in dichloromethane),[12] which also demonstrates the
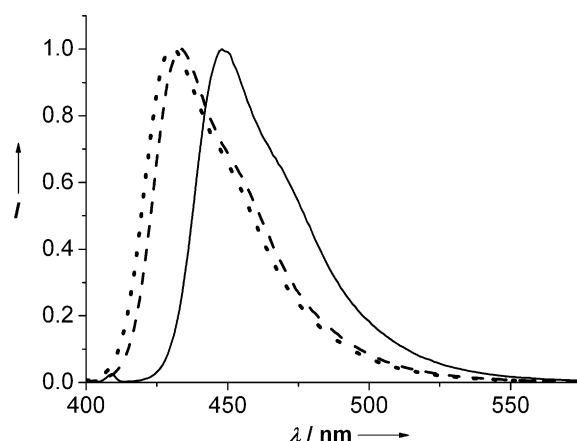


Figure 5. Normalized emission spectra of BOBTP$^m$ **3a** (dotted line), BOBTP$^m$ **3b** (dashed line), and BOBTP$^m$ **3c** (solid line) in dichloromethane.

important role of the substituents on the luminescent properties of BOBTPs. BOBTP$^p$ **4a** exhibited rather lower fluorescence quantum yield ($\Phi_F$ = 0.63 in cyclohexane) and molar extinction coefficient ($\varepsilon$ = 5600 M$^{-1}$cm$^{-1}$) than BOBTP$^m$ **3c**.
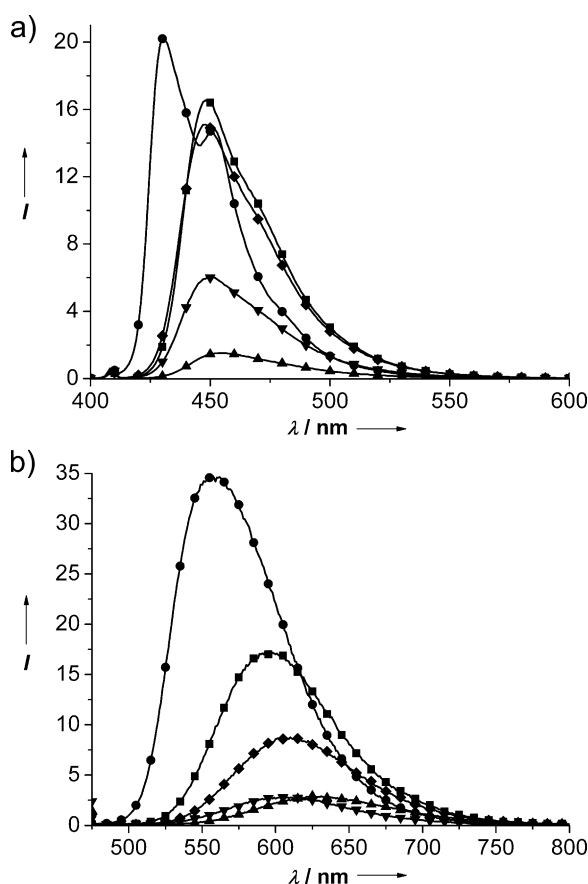
a)



b)



Figure 6. Electronic emission spectra of a) BOBTP$^m$ **3c** (10 μM) and b) BOBTP$^p$ **4a** (100 μM) in dichloromethane (■), cyclohexane (●), acetonitrile (▲), ethanol (▼), and tetrahydrofuran (◆).

Table 1. Photophysical data of BOBTPs in solution.

| | $\lambda_{abs}$ [nm] in CH$_2$Cl$_2$ | $\lambda_{em}$ [nm] in CH$_2$Cl$_2$ | Stokes shift [nm] | $\varepsilon$ [M$^{-1}$cm$^{-1}$] in CH$_2$Cl$_2$ | $\Phi_F$ in CH$_2$Cl$_2$ | $\Phi_F$ in cyclo-C$_6$H$_{12}$ |
|---|---|---|---|---|---|---|
| **3a** | 413 | 430 | 17 | 60 000 | 0.98[a] | 0.95[a] |
| **3b** | 417 | 434 | 17 | 66 000 | 0.96[a] | 0.93[a] |
| **3c** | 420 | 448 | 28 | 73 000 | 0.91[a] | 0.98[a] |
| **4a** | 456 | 597 | 141 | 5600 | 0.28[b] | 0.63[b] |

[a] 9,10-Diphenylanthracene was used as a reference dye ($\Phi_F$=0.90 in cyclohexane). [b] Fluorescein was used as a reference dye ($\Phi_F$=0.79 in 0.1 M aqueous NaOH).

**Theoretical calculations**: Computational calculations of the molecular orbitals for the boron complexes of BTPs (**4a**, **6**, and **3a**) suggest that the amino substituents increase both the HOMO and LUMO energies of the parent boron complex **6**, but to different degrees depending on the substitution position (Table 2).

In particular, the *para* derivative **4a** shows a significant increase in the HOMO energy (1 eV) with respect to the parent complex **6**, which is supported by the localized HOMO electron distribution (Figure 7). In the case of *meta* derivative **3a**, the perturbations in the HOMO and LUMO energy levels seem to be comparable in magnitude, and thus it shows the same bandgap as the parent complex **6** within computational errors.

Table 2. Calculated HOMO–LUMO energy states of BOBTPs **4a**, **6**, and **3a**.[a]

| | First ex. energy [eV] | $E$ (LUMO) [eV] | $E$ (HOMO) [eV] | $\Delta E$ [eV] |
|---|---|---|---|---|
| **4a** | 2.76 | −2.12 | −5.14 | 3.02 |
| **6** | 3.58 | −2.29 | −6.19 | 3.90 |
| **3a** | 3.63 | −1.82 | −5.48 | 3.66 |

[a] Calculations were done for the singlet ground state and for the first excited singlet state at the DFT level of theory using the hybrid exchange-correlation functional of Becke's three-parameter and the Lee–Yang–Parr approximation (B3LYP)[13] implemented in Spartan 08.[14]
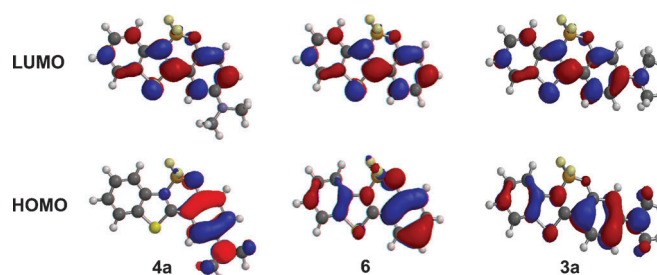


Figure 7. Theoretical electron distribution of the HOMO–LUMO energy states for complexes **4a**, **6**, and **3a**.

There is a clear difference in the electron distribution between the *para* complex **4a** and the *meta* complex **3a** (Figure 7). In the case of **4a**, the electron distribution in the HOMO is confined to the phenol moiety, whereas the electron distribution in the LUMO is shifted to the benzothiazole and the phenol ring. In contrast, the electron distribution in the HOMO and LUMO of **3a** does not show such a shift but shows a delocalized feature. The electron distribution shift observed in the case of the *para* substitution seems to cause a decrease in the quantum yield.

Experimental HOMO–LUMO energy gaps for the typical boron complexes were determined by X-ray photoelectron spectroscopy (XPS) in poly-(methyl methacrylate) (PMMA) film. We were able to obtain the HOMO energy levels for the *meta* derivative **3b** (−5.80 eV)[15] and the *para* derivative **4a** (−5.70 eV). From these data, the HOMO–LUMO energy gaps were determined to be 3.63 and 3.02 eV for **3b** and **4a**, respectively, based on the LUMO energies estimated by their maximum absorption wavelengths. These experimental HOMO–LUMO energy gaps match well with the computational values, as we expect similar values for **3a** (R′=Me) and **3b** (R′=Et).

**Solid-state luminescence**: BODIPY dyes typically show narrow emission spectra, an attractive feature for high color purity. Most of them, however, exhibit severe spectral overlap between the absorption and emission spectra on account of small Stokes shifts.[10] The spectral overlap leads to self-quenching of fluorescence at high concentration such as in the solid state. Furthermore, the π–π stacking in the solid

state, which is frequently observed for BODIPYs, leads to fluorescence quenching. Both undesirable features seem to limit the application of BODIPY dyes as OLED dopants, as indicated by a rare example.[16]

An approach of introducing bulky side substituents to BODIPY dyes has been explored to enlarge the Stokes shifts and thus to reduce the undesirable spectral overlap, and also to reduce the undesirable π–π stacking in the solid state.[17] This steric approach has been successful to some extent; however, the BODIPY derivatives thus developed by the steric approach still show considerable spectral overlap. An inherent problem in this steric approach arises, however, as larger Stokes shifts (larger structural changes upon excitation) would lead to more facile nonradiative decay of excitation energy, thus lowering the fluorescence quantum yield. Therefore, it is challenging to develop fluorescent dyes with high quantum yields by reducing the spectral overlap and the π–π stacking aggregation while maintaining narrow emission spectra.

To our delight, we found that our BOBTP dyes show bright luminescence even in the solid state. Both the *meta* and *para* complexes **3b** and **4a** in their crystal states show bright blue and red-orange luminescence, respectively, upon irradiation by UV light (Figure 8, top). Photos of the emis-
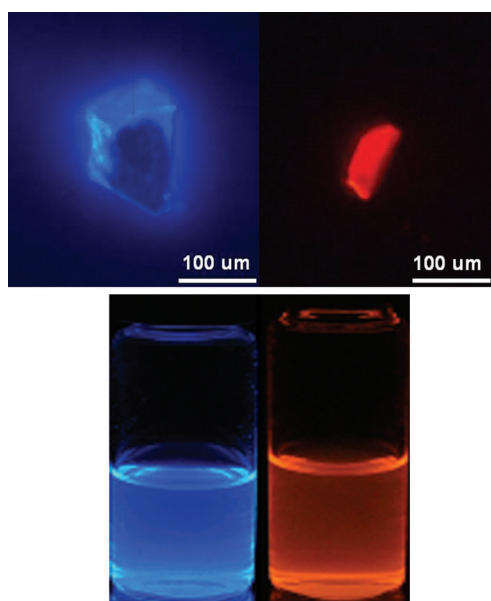


Figure 8. Top: Photos of luminescent crystals of **3b** (blue) and **4a** (orange-red) taken by irradiating with UV light in the range of 340–380 nm and 515–560 nm, respectively. Photos were magnified five times through a microscope. Bottom: Photos of emission colors of **3a** (blue) and **4a** (orange) in dichloromethane upon excitation at 395 and 450 nm, respectively.

sion colors of **3a** (blue) and **4a** (orange) in dichloromethane are provided for comparison (Figure 8, bottom). Organic small-molecule dyes have a propensity to lose their luminescence in the solid state, most probably on account of the ex-

citonic coupling that leads to quenching.[18] Many efforts have been made in the development of organic dye molecules that emit in the solid state, which have produced different types of solid dyes in the J aggregates.[19] BOBTP complexes thus constitute a new class of emitting compounds in the solid state.

Quantum yields were determined for the typical boron complexes (BOBTP$^m$ **3a** and **3b**, and BOBTP$^p$ **4a**) in the PMMA film by using a spectrometer based on the integrating sphere method. The results with Commission Internationale de l'Eclairage (International Commission on Illumination, or CIE) values are summarized in Table 3. The *meta*

Table 3. Photophysical data of BOBTPs in the solid state.

|  | $\lambda_{ex}$ [nm] | Absorbance | $\lambda_{em}$ [nm] | FWHM [nm] | $\Phi_F$ | CIE$_x$ | CIE$_y$ |
|---|---|---|---|---|---|---|---|
| **3a** | 413 | 0.88 | 449 | 40 | 0.85 | 0.15 | 0.08 |
| **3b** | 417 | 0.97 | 463 | 38 | 0.61 | 0.14 | 0.12 |
| **4a** | 456 | 0.72 | 598 | 99 | 0.43 | 0.27 | 0.15 |

derivative **3a** shows a high quantum yield of 0.85, whereas the *para* derivative **4a** shows a moderate quantum yield of 0.43. In the film state, the *meta* derivative **3a** shows a chromaticity value [CIE$_{x,y}$ (0.15, 0.08)], which is close to an ideal deep blue [CIE$_{x,y}$ (0.14, 0.08)].

**Crystal structures**: To gain a further understanding of why the boron complexes show strong luminescence in the solid state, we carried out X-ray crystal analysis for the single crystals obtained for BOBTP$^m$ **3b** and BOBTP$^p$ **4a**. We found that, in addition to the small spectral overlap, more importantly, there were few π–π stacking interactions in the solid state when we analyzed the crystal-packing patterns of **3b** and **4a**, respectively.[20] In the case of BOBTP$^m$ **3b**, of two parallel crystal planes observed, only one plane at a distance of 3.9 Å would have π–π interactions, if any (Figure 9a,c). In this case, however, there is little overlap between the two interlayered aromatic rings. The benzene rings of the phenol and the benzothiazole moieties do not show any overlap between themselves or between each other. Interestingly, the benzene rings overlap with the boron-chelated ring moiety that is not a π system. Therefore, BOBTP$^m$ dyes have low (in the case of **3c**) or small (in the cases of **3a** and **3b**) spectral overlap, if any, as well as little π–π stacking interactions in the solid state. These properties endow them with bright luminescence in the solid state.

The crystal-packing pattern of BOBTP$^p$ **4a**, which shows two orthogonal parallel layers (Figure 9b), also shows low π–π stacking interactions between the aromatic rings (Figure 9d). In this case, the benzene rings (the phenol and the benzothiazole moieties) also do not overlap with each other, but overlap with the boron-chelated ring moiety. Thus, **4a** also exhibits bright orange-red luminescence in the solid state on account of a bathochromic shift in the emission wavelength usually observed in the J-aggregated state.[19]
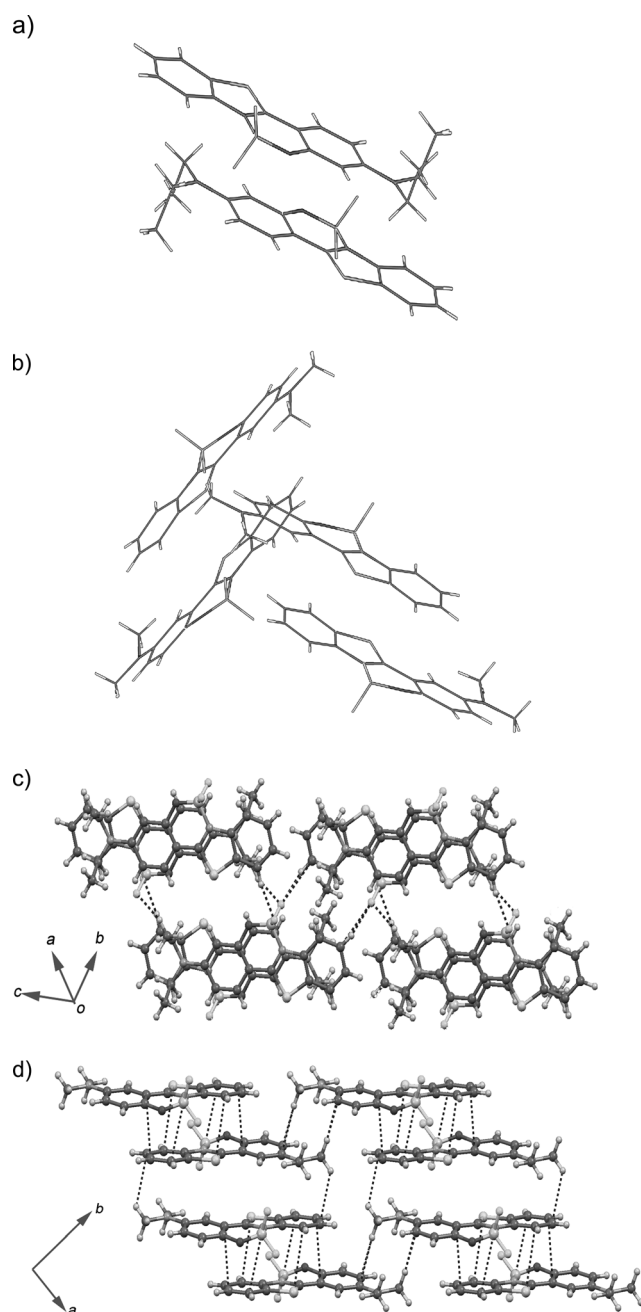
a)



b)



c)



d)



Figure 9. A part of a crystal-packing pattern of a) BOBTP$^m$ **3b** and b) BOBTP$^p$ **4a** that shows no stacking of the benzene rings between adjacent interlayered crystals; molecular packing of c) BOBTP$^m$ **3b** viewed along the *a* axis and d) BOBTP$^p$ **4a** viewed down the *c* axis in single crystals.

The solid structures suggest that such boron complexes are very promising as optoelectronic materials for OLEDs, lasers, field-effect transistors, and molecular probes.

**Electroluminescent properties**: Encouraged by the excellent luminescent properties of BOBTP complexes, and BOBTP$^m$ derivatives in particular, we evaluated their potential as OLED materials. A preliminary study on the electroluminescence properties of blue dye **3b** indicates that BOBTP$^m$

dyes have promising optoelectronic properties. A thermogravimetric analysis (TGA) for BOBTP$^m$ **3b** indicated that it is thermally stable up to 350 °C (see the Supporting Information). BOBTP$^m$ **3b** thus was spin-coated as a dopant into the emitting layer of an OLED with a configuration of indium oxide (ITO)/gradient hole injection layer (GraHIL; 50 nm)/poly[2,7-(9,9-di-*n*-octylfluorene)-*alt*-(1,4-phenylene-[(4-*sec*-butylphenyl)amino]-1,4-phenylene)] (TFB; 35–40 nm)/(4,4′-*N*,*N*′-dicarbazolyl)biphenyl (CBP; 40 nm)/2,2′,2″-(1,3,5-benzinetriyl)-tris(1-phenyl-1*H*-benzimidazole) (TPBi; 40 nm)/LiF (1 nm)/Al (130 nm).[21] GraHIL, TFB, CBP, and TPBi were used as the hole-transporting layer, interlayer, light-emitting layer, and electron-transporting layer, respectively. BOBTP$^m$ **3b** was spin-coated with CBP at a 3 wt % doping level. An energy diagram, photo- and electroluminescence spectra (Figure 10), a current den-
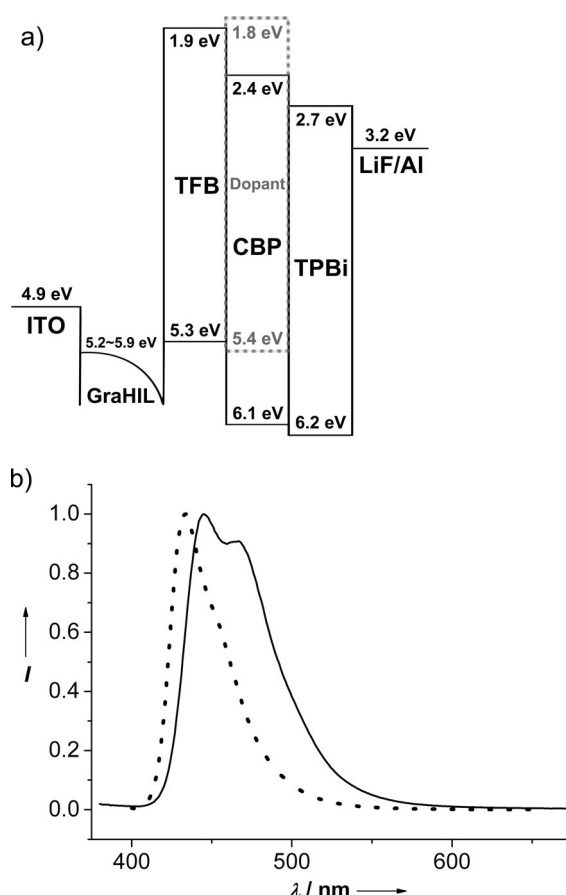


Figure 10. a) An energy diagram of the OLED device; b) normalized PL (dotted line) and EL (solid line) spectra of BOBTP$^m$ **3b**.

sity/voltage characteristic, and a luminance/voltage characteristic of the device (Figure 11) are provided.[22] A maximum brightness of 716 cd m$^{-2}$ was recorded at a driving voltage of 8.0 V. The chromaticity of the device at 4.9 V was CIE$_{x,y}$ (0.15, 0.11), which is close to an ideal deep blue [CIE$_{x,y}$ (0.14, 0.08)]. A peak current efficiency of 1.7 cd A$^{-1}$ was recorded at 3.0 V. These preliminary results are encour-
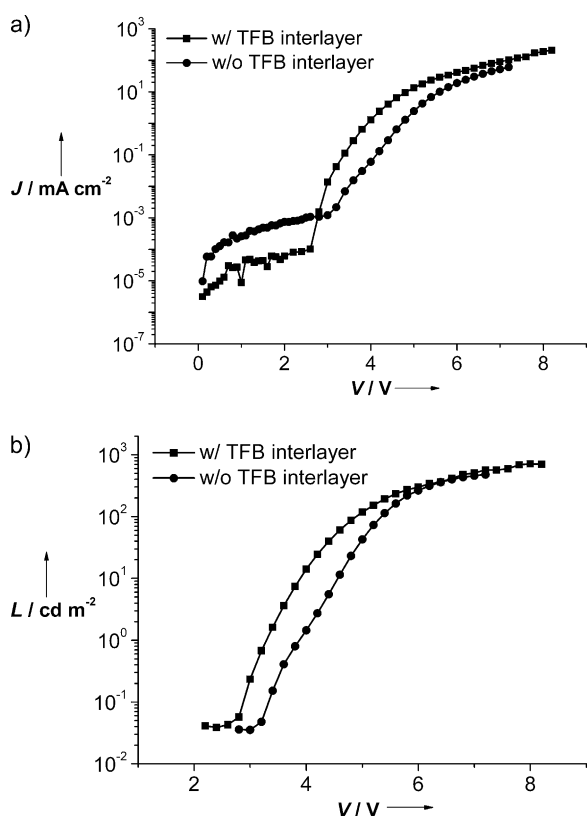
Figure 11. a) Current density versus voltage characteristic, and b) luminance versus voltage characteristic of the OLED device.

aging for further studies on optimal device characteristics based on boron complexes.

## Conclusion

We have demonstrated that substituents can induce dramatic changes in the photoluminescence properties of N,O-chelated boron complexes. Specifically, the boron complexes of 2-(benzothiazol-2-yl)phenols lead to bright deep blue- and orange-red-emitting materials depending on amino substituents at the 5- and 4-positions of 2-(benzothiazol-2-yl)phenol, respectively. Furthermore, both the boron complexes show bright luminescence in the solid state on account of low or small spectral overlap as well as the absence of $\pi$–$\pi$ stacking interactions in the solid state as analyzed by X-ray crystallography. A preliminary study indicates that the blue complexes have promising optoelectronic characteristics as dopants in an OLED device and show chromaticity close to an ideal deep blue. The substituent effects on the photoluminescent properties may be used to improve the photo- and electroluminescent properties of related boron complexes and also other metal complexes, both of which are under active investigation.

## Experimental Section

**Synthesis and characterization**: Synthesis of BTP **2a** (R′=Me) was carried out according to the reported procedure.[6] BTPs **3a**–**3c** were synthesized by a different route, and only characterization data for representative compounds are described here. Details can be found in the Supporting Information.

**BTP$^m$ 1a (R′=Et)**: $^1$H NMR (300 MHz, CDCl$_3$, 20°C, TMS): $\delta$=12.5 (s, 1H), 7.8–7.79 (m, 2H; Ar), 7.48–7.39 (m, 2H; Ar), 7.31–7.25 (m, 1H), 6.30–6.27 (m, 2H; Ar), 3.44–3.37 (q, $J$=7.2 Hz, 4H), 1.23–1.19 ppm (t, $J$=7.2 Hz, 6H); $^{13}$C NMR (75 MHz, CDCl$_3$, 20°C, TMS): $\delta$=169.7, 159.9, 152.4, 151.5, 132.1, 130, 126.4, 124.3, 121.3, 121.2, 106, 104.3, 98.1, 44.7, 12.8 ppm.

**BOBTP$^m$ 3a**: $^1$H NMR (300 MHz, CD$_2$Cl$_2$, 20°C, TMS): $\delta$=8.12–8.09 (m, 1H; Ar), 7.85–7.81 (m, 1H; Ar), 7.6–7.56 (m, 1H; Ar), 7.48–7.41 (m, 2H; Ar), 6.46–6.42 (dd, $J$=11.4, 2.4 Hz, 1H; Ar), 6.27 (d, $J$=2.4 Hz, 1H; Ar), 3.1 ppm (s, 6H); $^{13}$C NMR (125 MHz, CD$_2$Cl$_2$, 22°C, TMS): $\delta$= 168.1, 158, 156.8, 143.6, 128.5, 128.3, 128, 125.7, 122, 118.6, 106.4, 102.8, 98.7, 40.01 ppm (two carbon atoms); $^{19}$F NMR (300 MHz, CD$_2$Cl$_2$, 20°C, TFA): $\delta$=−61.63 ppm (q, $J$=16.50 Hz, 2F); $^{11}$B NMR (100 MHz, CD$_2$Cl$_2$, 20°C, BF$_3$·Et$_2$O): $\delta$=1.29–0.97 ppm (t, $J$=16 Hz, 1B).

**BOBTP$^m$ 3b**: $^1$H NMR (300 MHz, CDCl$_3$, 20°C, TMS): $\delta$=8.19–8.16 (m, 1H; Ar), 7.75–7.71 (m, 1H; Ar), 7.54–7.49 (m, 1H; Ar), 7.40–7.35 (m, 2H; Ar), 6.35–6.31 (dd, $J$=2.4, 9 Hz, 1H; Ar), 6.28–6.27 (d, $J$=2.4 Hz, 1H; Ar), 3.45–3.37 (q, $J$=7.2 Hz, 4H), 1.24–1.19 ppm (t, $J$=7.2 Hz, 6H); $^{13}$C NMR (75 MHz, CDCl$_3$, 20°C, TMS): $\delta$=167.5, 158.2, 154.6 (two carbon atoms), 134.5, 128.7, 128, 125.5, 121.6, 119, 106.2, 102.5, 98.5, 44.8, 12.6 ppm; $^{19}$F NMR (300 MHz, CDCl$_3$, 20°C, TFA): $\delta$=−137.8–138 ppm (q, $J$=18.6 Hz, 2F); $^{11}$B NMR (100 MHz, CDCl$_3$, 20°C, BF$_3$·Et$_2$O): $\delta$= 1.36–1.04 ppm (t, $J$=16 Hz, 1B).

**BOBTP$^p$ 4a**: $^1$H NMR (300 MHz, CDCl$_3$, 20°C, TMS): $\delta$=8.37–8.35 (d, $J$=8.1 Hz, 1H; Ar), 7.86–7.84 (d, $J$=8.1 Hz, 1H; Ar), 7.64–7.59 (m, 1H; Ar), 7.52–7.47 (m, 1H; Ar), 7.16–7.08 (m, 2H; Ar), 6.71–6.70 (d, $J$= 2.4 Hz, 1H; Ar), 2.93 ppm (s, 6H); $^{13}$C NMR (75 MHz, CD$_2$Cl$_2$, 22°C, TMS): $\delta$=170, 150, 144.7, 144.3, 130.1, 129.2, 127.6, 125.4, 122.8, 121.2, 120.6, 113.5, 109.3, 42.2 ppm (two carbon atoms); $^{19}$F NMR (300 MHz, CDCl$_3$, 20°C, TFA): $\delta$=−136.19–136.26 ppm (d, $J$=22.5 Hz, 2F); $^{11}$B NMR (100 MHz, CD$_2$Cl$_2$, 20°C, BF$_3$·Et$_2$O): $\delta$=1.50–1.20 ppm (t, $J$= 15 Hz, 1B).

CCDC-860065 (BOBTP$^m$ **3b**) and 860066 (BOBTP$^p$ **4a**) contain the supplementary crystallographic data for this paper. These data can be obtained free of charge from The Cambridge Crystallographic Data Centre via www.ccdc.cam.ac.uk/data_request/cif.

**OLED device fabrication**: Patterned ITO glass was cleaned by sonication in acetone and then in isopropanol, each for 15 min. The cleaned ITO glass was treated with UV/ozone for 15 min. The polymeric hole-injection layer (GraHIL) was blended with equal proportions of poly(3,4-ethylenedioxythiophene)/poly(4-styrenesulfonate) (PEDO-T/PSS) and a tetrafluoroethylene-perfluoro-3,6-dioxa-4-methyl-7-octenesulphonic acid copolymer (PFI). A 50 nm-thick GraHIL was spin-coated on the ITO under ambient conditions and baked immediately on a hot plate at 200°C for 15 min. A 35–40 nm-thick poly[2,7-(9,9-di-$n$-octylfluorene)-$alt$-(1,4-phenylene-[(4-$sec$-butylphenyl)amino]-1,4-phenylene)] (TFB) was used as interlayer, which was dissolved in toluene, spin-coated in a nitrogen glovebox, and annealed at 180°C for 30 min. The 40 nm-thick emitting layer (EML) was spin-coated on the TFB interlayer and annealed at 80°C for 30 min. The EML was composed of (4,4′-N,N′-dicarbazolyl)-biphenyl (CBP) as a host and BOBTP$^m$ **3b** as a dopant (3 wt%). Other layers were vacuum-deposited under a base pressure of $5 \times 10^{-7}$ torr without breaking the vacuum. As an electron-transport layer, 2,2′,2′′-(1,3,5-benzinetriyl)-tris(1-phenyl-1H-benzimidazole) (TPBi) was deposited on the EML to a 40 nm thickness. Lithium fluoride (1 nm) and aluminum (130 nm) were used for cathode layers. Devices were encapsulated by hollow glass and active area of OLED was 6 mm$^2$. The fabricated devices were measured using a Keathley 236 (measurement source) instrument, and a CS2000 (Konica Minolta) instrument was used for measuring the

current/voltage/luminance ($I$–$V$–$L$) characteristics and electroluminescence (EL) spectra.

## Acknowledgements

[1] a) G. Ulrich, R. Ziessel, A. Harriman, *Angew. Chem.* **2008**, *120*, 1202–1219; *Angew. Chem. Int. Ed.* **2008**, *47*, 1184–1201; b) R. Ziessel, G. Ulrich, A. Harriman, *New J. Chem.* **2007**, *31*, 496–501.

[2] A. Loudet, K. Burgess, *Chem. Rev.* **2007**, *107*, 4891–4932.

[3] BODIPY, short for boron–dipyrromethene, represents the boron complexes of dipyrromethenes; its use for the boron complexes based on other types of ligands should be avoided.

[4] a) S.-F. Liu, Q. Wu, H. L. Schmider, H. Aziz, N.-X. Hu, Z. Popović, S. Wang, *J. Am. Chem. Soc.* **2000**, *122*, 3671–3678; b) Y. Li, Y. Liu, W. Bu, J. Guo, Y. Wang, *Chem. Commun.* **2000**, 1551–1552; c) Y. Liu, J. Guo, H. Zhang, Y. Wang, *Angew. Chem.* **2002**, *114*, 190–192; *Angew. Chem. Int. Ed.* **2002**, *41*, 182–184; d) Q. Liu, M. S. Mudadu, H. Schmider, R. Thummel, Y. Tao, S. Wang, *Organometallics* **2002**, *21*, 4743–4749; e) H.-Y. Chen, Y. Chi, C.-S. Liu, J-K. Yu, Y.-M. Cheng, K.-S. Chen, P.-T. Chou, S.-M. Peng, G.-H. Lee, A. J. Carty, S.-J. Yeh, C.-T. Chen, *Adv. Funct. Mater.* **2005**, *15*, 567–574; f) T.-R. Chen, R.-H. Chien, M.-S. Jan, A. Yeh, J.-D. Chen, *J. Organomet. Chem.* **2006**, *691*, 799–804; g) H. Zhang, C. Huo, K. Ye, P. Zhang, W. Tian, Y. Wang, *Inorg. Chem.* **2006**, *45*, 2788–2794; h) Y. Zhou, Y. Xiao, D. Li, M. Fu, X. Qian, *J. Org. Chem.* **2008**, *73*, 1571–1574; i) Y. Zhou, Y. Xiao, S. Chi, X. Qian, *Org. Lett.* **2008**, *10*, 633–636; j) H.-J. Son, W.-S. Han, K.-R. Wee, J.-Y. Chun, K.-B. Choi, S. J. Han, S.-N. Kwon, J. Ko, C. Lee, S. O. Kang, *Eur. J. Inorg. Chem.* **2009**, 1503–1513; k) Y. Zhou, J. W. Kim, R. Nandhakumar, M. J. Kim, E. Cho, Y. S. Kim, Y. H. Jang, C. Lee, S. Han, K. M. Kim, J.-J. Kim, J. Yoon, *Chem. Commun.* **2010**, *46*, 6512–6514; l) Y. Zhou, J. W. Kim, M. J. Kim, W.-J. Son, S. J. Han, H. N. Kim, S. Han, Y. Kim, C. Lee, S.-J. Kim, D. H. Kim, J.-J. Kim, J. Yoon, *Org. Lett.* **2010**, *12*, 1272–1275; m) D. Frath, S. Azizi, G. Ulrich, P. Retailleau, R. Ziessel, *Org. Lett.* **2011**, *13*, 3414–3417; n) J. F. Araneda, W. E. Piers, B. Heyne, M. Parvez, R. McDonald, *Angew. Chem.* **2011**, *123*, 12422–12425; *Angew. Chem. Int. Ed.* **2011**, *50*, 12214–12217; o) J. Massue, D. Frath, G. Ulrich, P. Retailleau, R. Ziessel, *Org. Lett.* **2012**, *14*, 230–233.

[5] M. Santra, B. Roy, K. H. Ahn, *Org. Lett.* **2011**, *13*, 3422–3425.

[6] Wang and co-workers concurrently pursued similar substituent effects on the luminescent properties of the BTP ligands themselves: D. Yao, S. Zhao, J. Guo, Z. Zhang, H. Zhang, Y. Liu, Y. Wang, *J. Mater. Chem.* **2011**, *21*, 3568–3570.

[7] E. Barni, P. Savarino, M. Marzona, M. Piva, *J. Heterocycl. Chem.* **1983**, *20*, 1517–1521.

[8] During the publication process of this work, other groups also observed similar substituent effects for related diphenylboron complexes; they focused on the less bright *para* derivatives: D. Li, H. Zhang, C. Wang, S. Huang, J. Guo, Y. Wang, *J. Mater. Chem.* **2012**, *22*, 4319–4328.

[9] BOBTP represents the boron complex of 2-(benzothiazol-2-yl)phenol, the nomenclature of which is 6,6-difluoro-6-bora-5-oxa-11-thia-6a-aza-benzo[*a*]fluorine.

[10] R. Y. Lai, A. J. Bard, *J. Phys. Chem. B* **2003**, *107*, 5036–5042.

[11] S. Hamai, F. Hirayama, *J. Phys. Chem.* **1983**, *87*, 83–89.

[12] M. J. Kwak, Y. Kim, *Bull. Korean Chem. Soc.* **2009**, *30*, 2865–2866.

[13] A. Becke, *J. Chem. Phys.* **1993**, *98*, 5648–5652.

[14] *Spartan'08*, Wavefunction, Inc. Irvine, CA.

[15] The XPS measurement in the film state was not possible in the case of **3a** due to its low solubility.

[16] A. Hepp, G. Ulrich, R. Schmechel, H. von Seggern, R. Ziessel, *Synth. Met.* **2004**, *146*, 11–15.

[17] a) G. Ulrich, C. Goze, M. Guardigli, A. Roda, R. Ziessel, *Angew. Chem.* **2005**, *117*, 3760–3764; *Angew. Chem. Int. Ed.* **2005**, *44*, 3694–3698; b) D. Zhang, Y. Wen, Y. Xiao, G. Yu, Y. Liu, X. Qian, *Chem. Commun.* **2008**, 4777–4779; c) T. T. Vu, S. Badré, C. Dumas-Verdes, J.-J. Vachon, C. Julien, P. Audebert, E Yu. Senotrusova, E. Yu. Schmidt, B. A. Trofimov, R. B. Pansu, G. Clavier, R. Méallet-Renault, *J. Phys. Chem. C* **2009**, *113*, 11844–11855 and references therein; d) T. Ozdemir, S. Atilgan, I. Kutuk, L. T. Yildirim, A. Tulek, M. Bayindir, E. U. Akkaya, *Org. Lett.* **2009**, *11*, 2105–2107; e) G.-L. Fu, H. Pan, Y.-H. Zhao, C.-H. Zhao, *Org. Biomol. Chem.* **2011**, *9*, 8141–8146.

[18] M. Kasha, H. R. Rawls, M. A. El-Bayoumi, *Pure Appl. Chem.* **1965**, *11*, 371–392.

[19] a) D. G. Whitten, *Acc. Chem. Res.* **1993**, *26*, 502–509; b) K. C. Hannah, B. A. Armitage, *Acc. Chem. Res.* **2004**, *37*, 845–853; c) J. Lou, Z. Xie, J. W. Y. Lam, L. Cheng, H. Chen, C. Qiu, H. S. Kwok, X. W. Zhan, Y. Q. Liu, D. B. Zhu, B. Z. Tang, *Chem. Commun.* **2001**, 1740–1741; d) A. P. H. J. Schenning, P. Jonkheijm, E. Peeters, E. W. Meijer, *J. Am. Chem. Soc.* **2001**, *123*, 409–416; e) B. K. An, S. K. Kwon, S. D. Jung, S. Y. Park, *J. Am. Chem. Soc.* **2002**, *124*, 14410–14415; f) S. J. Toal, K. A. Jones, D. Magde, W. C. Trogler, *J. Am. Chem. Soc.* **2005**, *127*, 11661–11665; g) A. Dreuw, J. Plötner, L. Lorenz, J. Wachtveitl, J. E. Djanhan, J. Brüning, T. Metz, M. Bolte, M. U. Schmidt, *Angew. Chem.* **2005**, *117*, 7961–7964; *Angew. Chem. Int. Ed.* **2005**, *44*, 7783–7786; h) C. J. Bhongale, C. S. Hsu, *Angew. Chem.* **2006**, *118*, 1432–1436; *Angew. Chem. Int. Ed.* **2006**, *45*, 1404–1408; i) H. Tong, Y. Q. Dong, M. Häußler, J. W. Y. Lam, H. H.-Y. Sung, I. D. Williams, J. Sun, B. Z. Tang, *Chem. Commun.* **2006**, 1133–1135; j) E. Da Como, M. A. Loi, M. Murgia, R. Zamboni, M. Muccini, *J. Am. Chem. Soc.* **2006**, *128*, 4277–4281.

[20] Crystal data for BOBTP$^m$ **3b** ($C_{17}H_{17}BF_2N_2OS$): $M_r$ = 346.20; triclinic, space group $P\bar{1}$ (no. 2); $a$ = 8.5043(2), $b$ = 8.8157(2), $c$ = 12.0205(3) Å; $\alpha$ = 71.629(2), $\beta$ = 76.751(2), $\gamma$ = 68.273(2)°; $V$ = 788.01(3) Å$^3$; $Z$ = 2; $T$ = 100(2) K; $\mu(\lambda$ = 0.71073 Å) = 0.233 mm$^{-1}$; $\rho_{calcd}$ = 1.459 g cm$^{-3}$; 71 806 reflections measured, 12 373 unique ($R_{int}$ = 0.0793), $R_1$ = 0.0548, $wR_2$ = 0.1376 ($I$ > $2\sigma(I)$), $R_1$ = 0.0971, $wR_2$ = 0.1686 (all data); GOF = 1.022. Crystal data for BOBTP$^p$ **4a** ($C_{15}H_{13}BF_2N_2OS$): $M_r$ = 318.14; monoclinic, space group $P2_1/c$ (no. 14); $a$ = 8.5412(2), $b$ = 11.7529(3), $c$ = 13.8346(4) Å; $\beta$ = 102.157(2)°; $V$ = 1357.63(6) Å$^3$; $Z$ = 4; $T$ = 100(2) K; $\mu(\lambda$ = 0.71073 Å) = 0.263 mm$^{-1}$; $\rho_{calcd}$ = 1.557 g cm$^{-3}$; 89 916 reflections measured, 6997 unique ($R_{int}$ = 0.0830), $R_1$ = 0.0570, $wR_2$ = 0.1643 ($I$ > $2\sigma(I)$), $R_1$ = 0.1025, $wR_2$ = 0.1902 (all data); GOF = 1.108.

[21] ITO/GraHIL (50 nm)/TFB (35–40 nm)/CBP (40 nm)/TPBi (40 nm)/LiF (1 nm)/Al (130 nm). ITO: indium tin oxide. GraHIL: gradient hole injection layer (T.-W. Lee, Y. Chung, O. Kwon, J.-J. Park, *Adv. Funct. Mater.* **2007**, *17*, 390–396; T.-H. Han, Y. Lee, M.-R. Choi, S.-H. Woo, S.-H. Bae, B. H. Hong, J.-H. Ahn, T.-W. Lee, *Nat. Photonics* **2012**, *6*, 105–110). TFB: poly[2,7-(9,9-di-*n*-octylfluorene)-*alt*-(1,4-phenylene-[(4-*sec*-butylphenyl)amino]-1,4-phenylene)]. CBP: (4,4′-*N*,*N*′-dicarbazolyl)biphenyl (S. H. Kim, J. Jang, J. Y. Lee, *Appl. Phys. Lett.* **2007**, *90*, 223505). TPBi: 2,2′,2″-(1,3,5-benzinetriyl)-tris(1-phenyl-1*H*-benzimidazole) (Y. Byun, Y.-Y. Lyu, R. R. Das, O. Kwon, T.-W. Lee, *Appl. Phys. Lett.* **2007**, *91*, 211106).

[22] Since the TFB interlayer allows holes to be easily transported to the emitting layer, the device becomes more hole-dominant. Although the TFB interlayer lowers the operating voltage by transporting more holes to the emitting layer, the lower external quantum efficiency of the device with interlayer than that without interlayer may be caused by reduced balance of hole and electrons in the emitting layer.
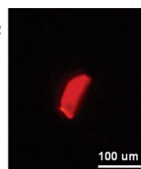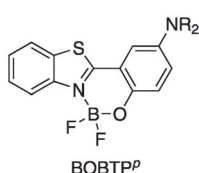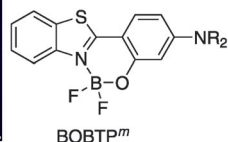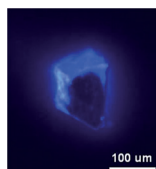
**The rainbow connection**: Boron complexes of 2-(benzothiazol-2-yl)phenols emit bright deep-blue or orange-red in solution and in solid states, depending on the position of amino substituents (see figure). Analyses reveal that the boron complexes show little or small absorption–emission spectral overlap and the absence of π–π stacking interaction in the crystal packing structures, respectively.

**Dramatic Substituent Effects on the Photoluminescence of Boron Complexes of 2-(Benzothiazol-2-yl)phenols**